Bioorg. Med. Chem. 36 (2021) 116094

Contents lists available at ScienceDirect

Bioorganic & Medicinal Chemistry

journal homepage: www.elsevier.com/locate/bmc

Structural modifications on indole and pyrimidine rings of osimertinib lead to high selectivity towards L858R/T790M double mutant enzyme and potent antitumor activity

Qiao Liu [a], Yanli Luo [a], Zerui Li [a], Chen Chen [b], Lei Fang [a,*]

[a] Jiangsu Province Hi-Tech Key Laboratory for Bio-medical Research, School of Chemistry and Chemical Engineering, Southeast University, Nanjing 211189, China
[b] School of Biology and Chemical Engineering, Jiangsu University of Science and Technology, Zhenjiang 212018, China

ARTICLE INFO

Keywords:
Osimertinib derivatives
Double mutant EGFR inhibitors
Selectivity

ABSTRACT

EGFR inhibitors represent a significant milestone for treatment of non-small cell lung cancer, however, they suffer from the acquired drug resistance. Utilizing osimertinib as the lead compound, this work has explored the structural modifications on the indole and pyrimidine rings of osimertinib to generate novel osimertinib derivatives. The *in vitro* enzymatic and cellular studies showed that the derivatives possessed high selectivity towards double mutant EGFR and potent antitumor activity. Particularly, compound **6b-1**, the most active compound, exhibited excellent inhibitory activity against double mutant EGFR (IC_{50} = 0.18 nM) and wild-type EGFR (IC_{50} = 2.89 nM) as well as H1975 cells (IC_{50} = 1.44 nM). Western blot analysis showed that **6b-1** completely inhibited double mutant EGFR and Erk phosphorylation. *In vivo* test using xenograft model indicated that compound **6b-1** had better antitumor efficacy than osimertinib. More importantly, **6b-1** displayed many advantages in the pharmacokinetic study, including better oral bioavailability and metabolism character.

1. Introduction

The discovery of the epidermal growth factor receptor (EGFR) tyrosine kinase inhibitors (TKIs), such as gefitinib, erlotinib and afatinib, based on the identification of EGFR activating mutations represent a significant milestone for treatment of non-small cell lung cancer (NSCLC), as well as for personalized medicine in oncology.[1] Although the first-generation (gefitinib/erlotinib) and second-generation (afatinib) EGFR TKIs have shown clinical superiority versus chemotherapy in treatment of EGFR mutant patients in terms of response rate, progression free survival (PFS), overall survival (OS) and quality of life of patients, it's unfortunate that almost all patients who initially respond to gefitinib/erlotinib and afatinib eventually acquire resistance to these drugs due to multiple molecular mechanisms:(a) EGFR target alteration; (b) activation of bypass mechanisms; and (c) phenotypic transformation to small cell lung cancer, or epithelial to mesenchymal transition (EMT).[2,3] By far, T790M mutation within exon 20 of EGFR gene is the most common mechanism of acquired resistance to the first- and second-generation EGFR TKIs, which has been first identified as a methionine replace the threonine at the 790 "gatekeeper" regulatory position of the EGFR kinase in 2005 by Kobayashi and co-workers.[4] The change of 790 amino acid residue not only leads to a steric hindrance that may interfere with TKI binding and increase of ATP affinity, but also can trigger other oncogenic signals, such as the β-catenin pathway.[5] Many efforts had been made to develop the third-generation EGFR TKIs to overcome resistance result from T790 mutation before a major breakthrough occurred in 2009 with the discovery of a novel class of covalent pyrimidine EGFR TKIs represented by osimertinib (AstraZeneca, peviously known as mereletinib or AZD9291)[6,7] and rociletinib (Clovis Oncology, formerly named CO-1686)[8] (Fig. 1). Osimertinib has been granted accelerated approval with a companion diagnostic for EGFR-T790 by the United States Food and Drug Administration (FDA) based on results of the phase I trial (AURA study) and an ongoing phase II trial of osimertinib 80 mg daily for EGFR-T790M mutation-positive lung adenocarcinomas (AURA2 study) in November 2015. The European Medicines Agency (EMA) gave a similar approval in Feb 2016 after two phase II studies (AURA extension and AURA2). Secondary acquired resistance to osimertinib and rociletinib has already emerged after the patients were treated for 8–10 months. In addition, in human pharmacokinetic study of osimertinib, the main metabolite AZ5104 and AZ7550, appeared to possess similar double and activating mutant potency to osimertinib, as well as high wild type inhibitory activity, leading to a poor *in vivo*

* Corresponding author.
E-mail address: lei.fang@seu.edu.cn (L. Fang).

https://doi.org/10.1016/j.bmc.2021.116094
Received 6 December 2020; Received in revised form 15 February 2021; Accepted 19 February 2021
Available online 25 February 2021

selectivity and diminish margins to EGFRi driven wild type toxicity,[9,10] which means that raising dose to increase the competition to ATP in case of C797S mutation will be impossible. To overcome these limits plenty of novel pyrimidine derivatives have been developed to explore their potential as antitumor agents, such as the *1H*-pyrazolo[3,4–*d*]pyrimidine derivatives and the thieno[2,3-*d*]pyrimidine derivatives.[11,12]

We are concerned about *in vivo* possible toxicity of the third generation EGFR TKIs and pursue more *in vivo* selectivity potency agents with wider therapeutic window. Analyzing the structure-activity relationship of osimertinib,[13,14] we found that the pyrimidine core plays important roles in the interaction with the kinase hinge and the indole group is responsible for the action on the back pocket region of the kinase. Particularly, the acrylamide moiety was therefore in a manner that could target Cys-797 and form a covalent bond (Fig. 1). More importantly, osimertinib was mainly metabolized on the indole ring to give the demethylation metabolite AZ5104, which leads to a poor *in vivo* selectivity and high toxicity. With this knowledge in mind, we performed structural modifications on the indole and the pyrimidine rings of osimertinib. As the indole *N*-methyl group and the 5-substituent of the pyrimidine ring of osimertinib had dramatic impact on double mutant potency and selectivity from wild type EGFR and IGFIR, which influences insulin receptor signals, we replaced the methyl on the indole 1-position and/or introduced a trifluoromethyl group at the 5-position of osimertinib, resulting in a set of analogues to osimertinib (Fig. 1). Furthermore, we also have interest to investigate how the structural modification influences the metabolic products.

2. Results and discussions

2.1. Chemistry

The compounds were prepared following the literature strategy outlined in Scheme 1.[6] Initially, the indole displacement was conducted by the treatment of the commercially accessible pyrimidine derivatives with equal molar MeMgBr and indole. The mechanism of this reaction is probably that the indole was firstly deprotonated with methylmagnesium bromide and subsequent connected to the pyrimidine ring via nucleophilic aromatic substitution reaction (S_NAr).[15] For the modification on the indole 1-position, alkyl group was introduced by the treatment of iodide or bromide compounds under the basic condition. The dimethylsulfamoyl displacement was performed by treating the intermediate **1** with dimethylsulfamoyl chloride, while acetyl displacement with acetyl chloride. Then the aniline moiety and the diamine chain were introduced via a substitution reaction in turn. Thereafter, the nitro group was reduced and acrylamide was formed by the treatment of acryloyl chloride, giving the final products. The structures of the products were confirmed by ^{1}H NMR, ^{13}C NMR and HRMS. All the proton and carbon signals can be appointed based on the target structure, and the $[M+H]^+$ peak of each target compound can also be found in HRMS.

Reagents and conditions: a) MeMgBr (1.0 M in THF), indole, THF, 0–60 °C; b) alkyl displacement: R_2Br, NaH, DMF, 0-rt; dimethylsulfamoyl displacement: dimethylsulfamoyl chloride, NaH, DMF, 0 °C -rt; acetyl displacement: acetic anhydride, NEt_3, 120 °C; c) aniline, *p*-TSA, 2-pentanol, 120 °C; d) N,N,N′-trimethylethane-1,2-diamine, DMA, 140 °C; e) Pd/C, H_2 balloon, MeOH, rt; f) acryloyl chloride, DIPEA, THF, 0 °C.

2.2. Biochemical and cellular activity characterization

With a set of derivatives of osimertinib in hand, we first evaluated their potency of inhibition against the EGFR wild-type and L858R/T790M double-mutant enzymes using homogeneous time-resolved fluorescent kinase assays. As showed in Table 1, all of the target compounds showed pronounced inhibitory activity against DM enzyme, with the IC_{50} values ranging from 0.17 to 12.08 nM. Introduction of cycloalkyl groups or dimethylsulfamoyl group on the indole nitrogen afforded compounds **6a-2**, **6b-1** and **6b-5**, whose inhibition potency was significantly increased and the IC_{50} values reached 0.17, 0.18 and 0.20 nM, respectively, 2–3 fold lower than that of osimertinib. Interestingly, compound **6b-1** showed excellent activity against DM enzyme while its analogue **6a-1**, which bearing a CF_3 group on the pyrimidine scaffold instead of H, only showed relative weak activities to both DM and WT enzymes. Similar results were also observed when comparing the data of **6a-2** and **6b-7**, suggesting the trifluoromethyl group might not be optimal for the activity.

In order to further explore the binding mode as well as the structure-activity relationship of the target compound, **6b-1** was chosen for docking studies. As shown in Fig. 2 A1, osimertinib and **6b-1** had quite similar interaction mode with wild type EGFR (PDB code: 4ZAU). As for **6b-1**, its anilino part was oriented toward the solvent channel of the ATP pocket and formed additional hydrogen bonds to Lys745 and Glu742 (Fig. 2 A2). When the inhibitors were docked to T790M mutant EGFR (PDB code: 6JX4), we found that the aromatic core of **6b-1** interacted with Lys745 via conjugation effect. Besides, a hydrogen bond to Thr854 was also formed. In this binding mode, the substituent on the pyrimidine ring could also affect the methionine gatekeeper Met 790. Particularly, the acrylamide moiety was therefore in a manner that could exactly target Cys-797 and the formation of a covalent bond could be expected, which was just similar to osimertinib (Fig. 2 B1-2).

With the delight results in the enzymatic activity tests, the target compounds were then chosen to evaluate their antiproliferative activities against H1975 (the double mutant EGFR cells) and A431 (the wild type cells) cell lines using CellTiter-Glo assay. As demonstrated in Table 2, most of the tested compounds, except **6b-2** and **6b-6,** displayed potent cellular activities against the double mutant cells, with the IC_{50} values in the single digit nanomolar range. As for A431 cell line, all of the target compounds showed weak activity, thus offering a clear selectivity towards the double mutant EGFR cells. Again, compound **6b-**

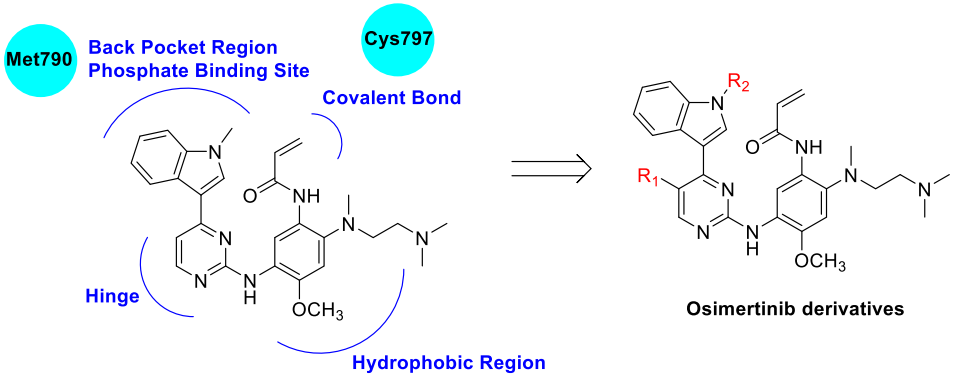

Fig. 1. The binding mode of osimertinib, and the structural modification leading to the derivatives.

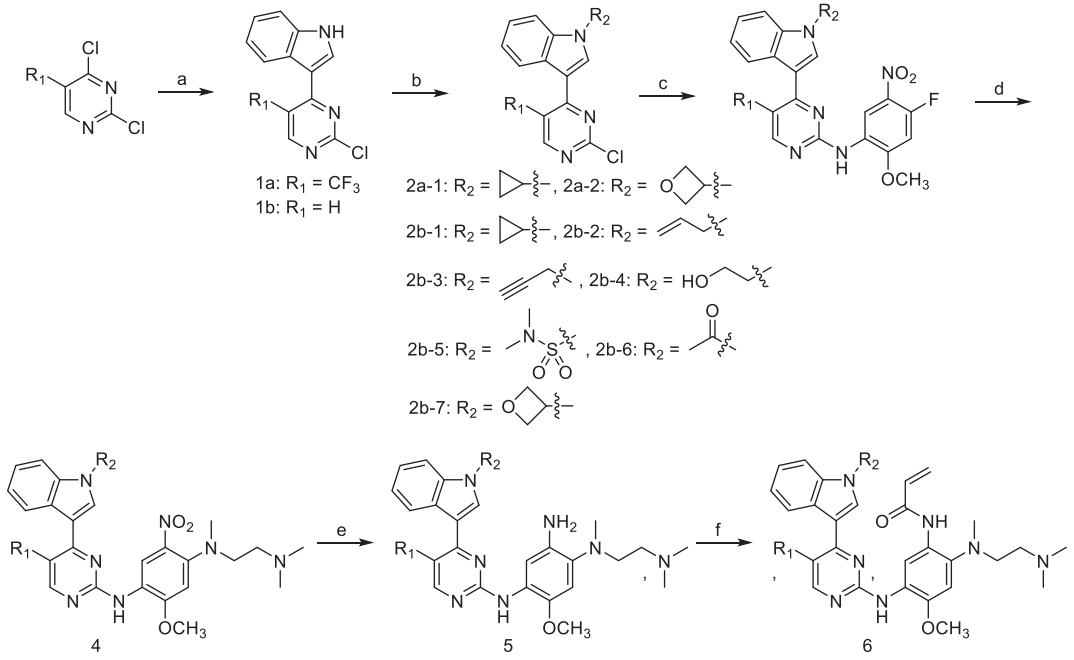

Scheme 1. General synthesis approach of 1 and/or 5 position replaced derivatives of osimertinib.

Table 1
Inhibitory activities of the analogues of osimertinib against the L858R/T790M double mutant (DM) and Wild-Type(WT) Enzymes.

Compounds				EGFR IC_{50} (nM)		
General Structure	Number	R1	R2	DM Enzyme	WT Enzyme	Selectivity
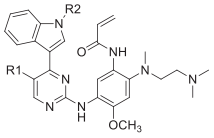	**6a-1**	CF_3		12.08 ± 1.50	50.58 ± 1.50	4.2
	6a-2	CF_3		0.17 ± 0.05	2.60 ± 0.50	15.3
	6b-1	H		0.18 ± 0.05	2.89 ± 1.20	16.1
	6b-2	H		1.51 ± 0.20	15.36 ± 1.55	10.2
	6b-3	H		1.01 ± 0.04	13.72 ± 0.60	13.7
	6b-4	H		0.86 ± 0.30	1.54 ± 0.10	1.8
	6b-5	H		0.20 ± 0.05	1.40 ± 0.25	7.0
	6b-6	H		2.09 ± 0.60	15.49 ± 2.05	7.4
	6b-7	H		0.95 ± 0.05	11.32 ± 0.50	11.9
	AZD9291	H	CH_3	0.55 ± 0.05	1.15 ± 0.12	2.1

1 was the most active one (IC_{50} 1.44 nM), whose potency was more than 10-fold higher than that of osimertinib against H1975 cells. Its IC_{50} value against A431 was 208.7 nM, thus the selectivity ratio reached 145, indicating **6b-1** was a good selective inhibitor towards the EGFR double mutant cells.

2.3. Western blot analysis

In addition to the enzymatic and cellular inhibition characterization, we selected four compounds to investigate their potential to inhibit the phosphorylation of EGFR as well as its downstream signaling pathways using western blot analysis (Fig. 3). Treatment of 3 nude mice with subcutaneous xenograft H1975 tumor with 5 mg tested compounds via single intragastric administration respectively, blood and tumor tissues were taken after 6 h to detect phosphorylated EGFR and the downstream phosphor-Akt and phosphor-Erk levels. To our delight, at a dose of 5 mg, **6a-1**, **6a-2**, **6b-1**, **and 6b-2** induced complete phosphorylation inhibition of double mutant EGFR. The downstream phosphor-Akt was reduced to the same extent accordingly attributed to **6b-1** and **6b-2**. Remarkably, **6b-1** also induced complete inhibition of phosphorylation of Erk. As compared to AZD9291, **6b-1** displayed the same activity.

2.4. Efficacy studies using in vivo xenograft model

Based on the obtained *in vivo* effects on the target protein in western blot analysis, **6b-1** was selected for further evaluation in efficacy studies using *in vivo* xenograft models representing H1975. AZD9291 was used as positive control. The substances were administered orally once a day for 11 days at a dose of 5 mg/kg. As shown in Fig. 4, 6b-1 displayed significant tumor growth inhibition. The tumor inhibiting rate of **6b-1** reached 83%, much higher than that of AZD9291 (70%). Besides, no obvious effect on the body weight was observed during the test, indicating **6b-1** had a good safety character.

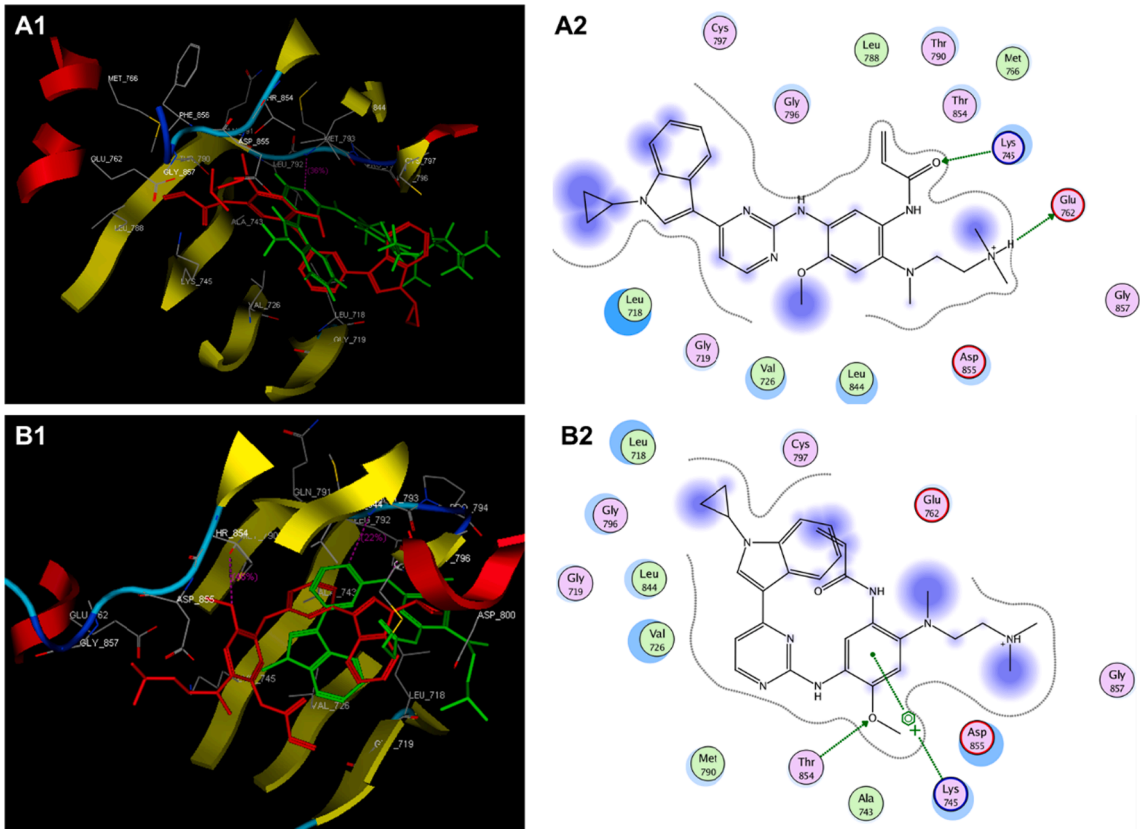

Fig. 2. A1: The overlap binding modes of **6b-1** (red) and osimertinib (green) to wild type EGFR (PDB code: 4ZAU). A2: The interaction illustration of 6b-1 with wild type EGFR. B1: The overlap binding modes of **6b-1** (red) and osimertinib (green) to T790M mutant EGFR (PDB code: 6JX4). B2: The interaction illustration of 6b-1 with T790M mutant EGFR.

Table 2
Antiproliferation assay of analogues of osimertinib.

Compounds				Antiproliferative IC_{50} (nM)		DM/WT Selectivity
General Structure	Number	R1	R2	H1975	A431	
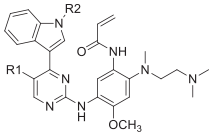	**6a-1**	CF_3		8.15 ± 1.05	59.05 ± 2.00	7.2
	6a-2	CF_3		1.45 ± 0.35	64.83 ± 3.00	45
	6b-1	H		1.44 ± 0.25	208.7 ± 18.0	145
	6b-2	H		33.99 ± 5.50	NT	NT
	6b-3	H		6.22 ± 1.15	690.0 ± 25.0	111
	6b-4	H		2.20 ± 0.05	208.4 ± 12.0	95
	6b-5	H		1.71 ± 0.25	26.03 ± 5.55	15
	6b-6	H		15.80 ± 2.00	191.6 ± 9. 5	12
	6b-7	H		9.44 ± 1.05	84.26 ± 7.50	8.9
	AZD9291	H	CH_3	18.21 ± 1.45	795.2 ± 25.5	44

2.5. Pharmacokinetic characterization

On the basis of encouraging *in vivo* results as well as *in vitro* activity against double mutant EGFR and selectivity over wild-type, we selected **6b-1** to further investigate full pharmacokinetic properties and its metabolic fate in rats. The obtained information is outlined in Table 3 and Fig. 4. Consistent with the reported literatures,[9,10] the metabolite analysis found that osimertinib was mainly metabolized to **7** (i.e. AZ5104) and **8** in plasma samples from rat, with lower concentrations than parent molecule. In contrast, for **6b-1**, only dealkylation in the N,N, N′-trimethylethylenediamine side chain, yielding **9**, was observed. This finding indicated that the diminishing selectivity and increase of toxic risk resulting from the metabolite would be avoided with **6b-1**. In addition, oral bioavailability of **6b-1** was about 6 times better than osimertinib.

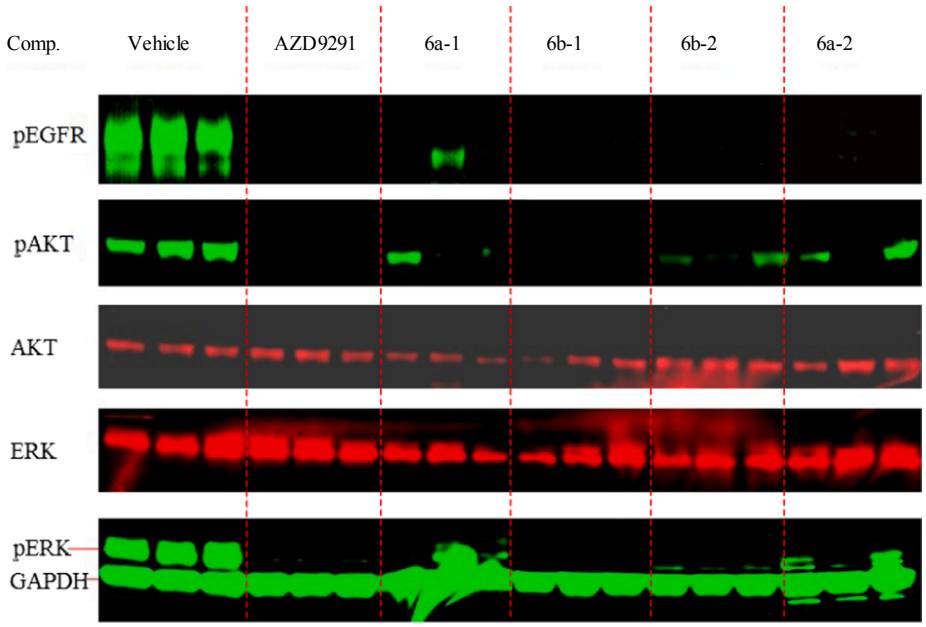

Fig. 3. Western blot analysis of inhibition of EGFR and downstream phosphorylation after treatment of nude mice with subcutaneous xenograft H1975 tumor with compound **6a-1**, **6a-2**, **6b-1**, **6b-2** at dose of 5 mg.

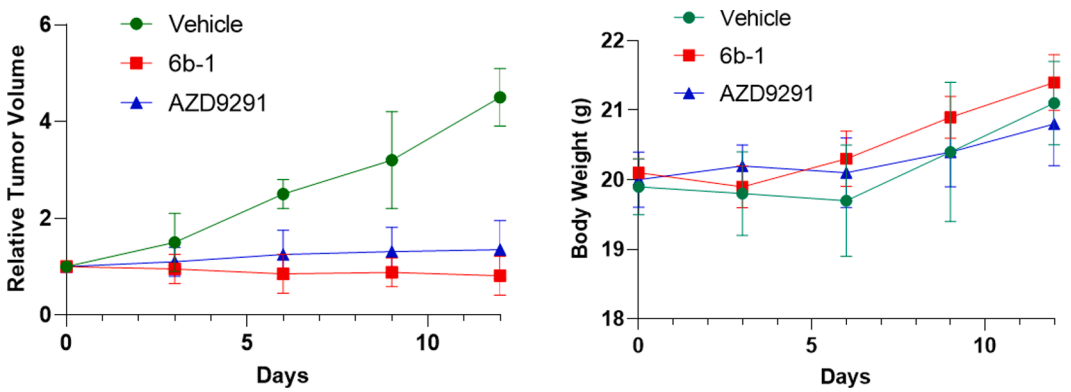

Fig. 4. Antitumor activity of compound **6b-1** on H1975 xenograft models. Nude mice implanted with H1975 cells in the flank were administered orally of **6b-1** (5 mg/kg), AZD9291 (5 mg/kg), vehicle (equivalent volume of normal saline injection) once a day for 11 days. The mice were sacrificed and made mathematical statistics. Left: The elative tumor volume (±SEM) was graphed with error bars representing the standard deviation. Right: The average body weights (±SEM) were plotted after sacrifice of the mice.

Table 3
In vivo pharmacokinetic parameters and metabolism for 6b-1 with AZD9291 as positive control.

Species	Major Parameters	AZD9291			6b-1	
		PM	7	8	PM	9
Rat	T_{max} (h)	1	6	NA	1	6
5 mg/Kg, po	C_{max} (ng/mL)	81.4	48.3	NA	528	126
	$AUC_{0\text{-}8}$ (ng/mL*h)	883	796	NA	4584	2062
	$AUC_{0\text{-}\infty}$ (ng/mL*h)	929	974	NA	5151	NA
	$T_{1/2}$ (h)	5.4	9.9	NA	7	NA
	$MRT_{0\text{-}\infty}$ (h)	9	14.1	NA	9.2	NA
	F (%)	9	NA	NA	52	NA

PM: parent molecule; NA: not analyzed or lower than detection limit.
Structures of 7, 8 and 9 were shown in Fig. 5.

3. Conclusions

In summary, we have reported the development a set of derivatives of osimertinib by structural modification on the indole 1-position and/or the 5-position of osimertinib. The derivatives could target to double mutant EGFR and show good selectivity over wild-type. The compounds with superior inhibitory activity against T790M resistant mutant EGFR and higher selectivity lead to improved therapeutic margin. In the *in vivo* test, compound **6b-1** showed better antitumor efficacy than osimertinib. More importantly, **6b-1** displayed many advantages in the pharmacokinetic study, including better oral bioavailability than osimertinib as well as metabolism character. As a result, **6b-1** could be considered as a potential candidate for further exploration.

4. Experiment section

4.1. Chemistry

Materials and instruments All chemicals were obtained from commercial purchase and solvents were purified and dried by standard procedures. Flash chromatography (FC): silica gel (SiO_2; 40 mm, 200–300 mesh). ^{1}H NMR and ^{13}C NMR Spectra: Bruker AVANCE III HD 600 MHz NMR Spectrometer. Mass spectra were measured by an Agilent 6224 ESI/TOF MS instrument.

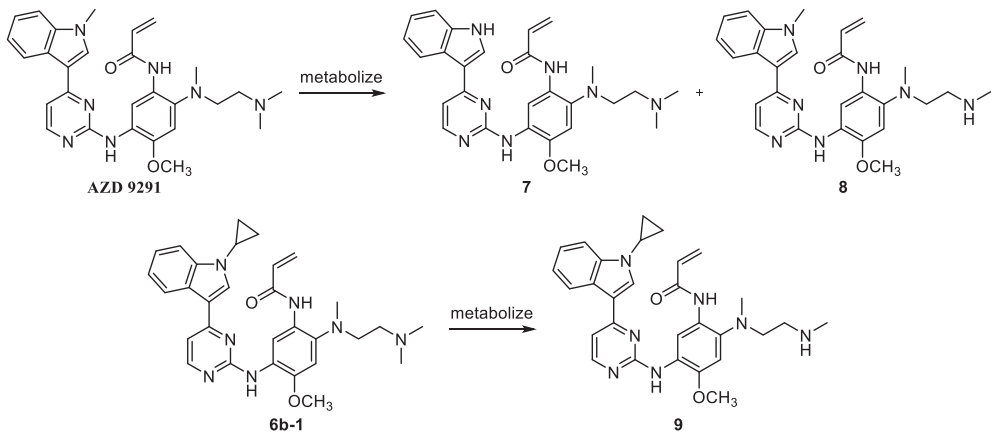

Fig. 5. Structures of metabolites of osimertinib and 6b-1.

*4.2. General procedure for the synthesis of compounds **2a-1, 2a-2, 2b-1∼2b-7***

Compound **1a** or **1b** (1 mmol) which prepared via a previously reported method[6] was dissolved in 20 mL of DMF. The solution was cooled to 0 °C and then NaH (4 mmol) was added. The obtained reaction mixture was stirred for 0.5 h, followed the addition of the corresponding R_2Br. After stirring at room temperature for 3 h, the reaction mixture was poured into 50 mL of ice-water and abstracted with ethyl acetate (25 mL × 3). The organic layer was dried, filtrated and concentrated under reduced pressure. Then the product was obtained via column chromatography (CH_2Cl_2: CH_3OH = 10: 1). For the dimethylsulfamoyl displacement, the procedure was the same but using dimethylsulfamoyl chloride instead of R_2Br as the reactant. For the acetyl displacement, 1a or 1b (1 mmol), acetic anhydride (1.5 mmol), NEt_3 (1.5 mmol) were dissolved in 20 mL of DMF. The solution was heated to 120 °C and stirred for 5 h. Then reaction mixture was poured into 50 mL of ice-water and abstracted with ethyl acetate (25 mL × 3). The organic layer was dried, filtrated and concentrated under reduced pressure. Then the product was obtained via column chromatography (CH_2Cl_2: CH_3OH = 10: 1).

3-(2-Chloro-5-(trifluoromethyl)pyrimidin-4-yl)-1-cyclopropyl-1H-indole (2a-1). Yield 62%, yellow oil. ^{1}HNMR (400 MHz, CD_3OD): δ 8.64 (s, 1H), 8.47–8.49 (m, 1H), 7.42 (s, 1H), 7.08–7.15 (m, 3H), 2.96 (m, 1H), 1.19–1.26 (m, 4H). ESI-MS: 338.1 $[M+H]^+$.

3-(2-Chloro-5-(trifluoromethyl)pyrimidin-4-yl)-1-(oxetan-3-yl)-1H-indole (2a-2). Yield 54%, yellow oil. ^{1}HNMR (400 MHz, CD_3OD): δ 8.86 (s, 1H), 8.44 (d, 1H), 7.71 (s, 1H), 7.32–7.25 (m, 3H), 5.02–4.96 (m, 4H), 4.82–4.84 (m, 1H). ESI-MS: 354.0 $[M+H]^+$.

3-(2-Chloropyrimidin-4-yl)-1-cyclopropyl-1H-indole (2b-1). Yield 68%, yellow oil. ^{1}HNMR (400 MHz, CD_3OD): δ 8.50 (d, 1H), 8.26 (d, 1H), 7.59 (s, 1H), 7.24 (d, 1H), 7.00–7.13 (m, 3H), 2.96–3.00 (m, 1H), 1.22–1.27 (m, 4H). ESI-MS: 270.0 $[M+H]^+$.

1-Allyl-3-(2-chloropyrimidin-4-yl)-1H-indole (2b-2). Yield 77%, yellow oil. ^{1}HNMR (400 MHz, CD_3OD): δ 8.72 (d, 1H), 8.34 (d, 1H), 7.96 (s, 1H), 7.45 (d, 1H), 7.22–7.33 (m, 3H), 6.00–6.03 (m, 1H), 5.34 (d, 1H), 5.23 (d, 1H), 4.68 (d, 2H). ESI-MS: 270.0 $[M+H]^+$.

3-(2-Chloropyrimidin-4-yl)-1-(prop-2-yn-1-yl)-1H-indole (2b-3). Yield 50%, yellow oil. ^{1}HNMR (400 MHz, CD_3OD): δ 8.77 (d, 1H), 8.31 (br, 1H), 7.82 (s, 1H), 7.36–7.39 (m, 2H), 7.18–7.21 (m, 2H), 4.94 (s, 2H), 2.33 (s, 1H). ESI-MS: 268.0 $[M+H]^+$.

2-(3-(2-Chloropyrimidin-4-yl)-1H-indol-1-yl)ethan-1-ol (2b-4). Yield 42%, yellow oil. ^{1}HNMR (400 MHz, CD_3OD): δ 8.73 (d, 1H), 8.23 (d, 1H), 7.86 (s, 1H), 7.43–7.45 (m, 2H), 7.28–7.30 (m, 1H), 7.12–7.15 (m, 1H), 4.29 (t, 2H), 3.74 (t, 2H). ESI-MS: 274.0 $[M+H]^+$.

3-(2-Chloropyrimidin-4-yl)-N,N-dimethyl-1H-indole-1-sulfonamide (2b-5). Yield 70%, yellow oil. ^{1}HNMR (400 MHz, CD_3OD): δ 8.70 (d, 1H), 8.21 (d, 1H), 8.08 (d, 1H), 7.66–7.69 (m, 2H), 7.39–7.41 (m, 2H), 2.79 (s, 6H). ESI-MS: 337.1 $[M+H]^+$.

1-(3-(2-Chloropyrimidin-4-yl)-1H-indol-1-yl)ethan-1-one (2b-6). Yield 62%, yellow oil. ^{1}HNMR (400 MHz, CD_3OD): δ 8.66 (d, 1H), 7.96–8.01 (m, 2H), 7.78 (s, 1H), 7.66 (d, 1H), 7.42–7.50 (m, 2H), 2.58 (s, 3H). ESI-MS: 272.1 $[M+H]^+$.

3-(2-Chloropyrimidin-4-yl)-1-(oxetan-3-yl)-1H-indole (2b-7). Yield 60%, yellow oil. ^{1}HNMR (400 MHz, CD_3OD): δ 8.73 (d, 1H), 8.22 (d, 1H), 7.88 (s, 1H), 7.43 (d, 1H), 7.19–7.28 (m, 3H), 4.92–4.96 (m, 4H), 4.84–4.86 (m, 1H). ESI-MS: 286.0 $[M+H]^+$.

*4.3. General procedure for the synthesis of compounds **3a-1, 3a-2, 3b-1∼3b-7***

Compound **2** (1 mmol) and 4-fluoro-2-methoxy-5-nitroaniline (1 mmol) were dissolved in 20 mL of 2-pentanol to which catalytic amount of p-TSA was added. The solution was heated to 120 °C and kept stirring for 3 h. The reaction solution was then cooled to room temperature and the product was obtained via column chromatography (CH_2Cl_2: CH_3OH = 10: 1).

4-(1-Cyclopropyl-1H-indol-3-yl)-N-(4-fluoro-2-methoxy-5-nitrophenyl)-5-(trifluoromethyl) pyrimidin-2-amine (3a-1). Yield 65%, yellow oil. ^{1}HNMR (400 MHz, CD_3OD): δ 8.51–8.53 (m, 2H), 7.89 (s, 1H), 7.06–7.17 (m, 5H), 3.70 (s, 3H), 2.96–3.00 (m, 1H), 1.19–1.27 (m, 4H). ESI-MS: 488.1 $[M+H]^+$.

***N*-(4-Fluoro-2-methoxy-5-nitrophenyl)-4-(1-(oxetan-3-yl)-1H-indol-3-yl)-5-(trifluoromethyl) pyrimidin-2-amine (3a-2).** Yield 60%, brown foam. ^{1}HNMR (400 MHz, CD_3OD): δ 8.73 (s, 1H), 8.49 (d, 1H), 7.86 (s, 1H), 7.46 (s, 1H), 7.25–7.35 (m, 2H), 7.08–7.12 (m, 2H), 4.96–4.98 (m, 1H), 4.84–4.88 (m, 4H), 3.66 (s, 3H). ESI-MS: 504.1 $[M+H]^+$.

4-(1-Cyclopropyl-1H-indol-3-yl)-N-(4-fluoro-2-methoxy-5-nitrophenyl)pyrimidin-2-amine (3b-1). Yield 54%, orange foam. ^{1}HNMR (400 MHz, CD_3OD): δ 8.28 (d, 1H), 8.11 (s, 1H), 7.89 (s, 1H), 7.34 (s, 1H), 7.05–7.15 (m, 3H), 7.01–7.03 (m, 2H), 3.70 (s, 3H), 2.96–2.99 (m, 1H), 1.19–1.27 (m, 4H). ESI-MS: 420.1 $[M+H]^+$.

4-(1-Allyl-1H-indol-3-yl)-N-(4-fluoro-2-methoxy-5-nitrophenyl) pyrimidin-2-amine (3b-2). Yield 60%, brown foam. ^{1}HNMR (400 MHz, CD_3OD): δ 8.33–8.39 (m, 2H), 7.82 (s, 1H), 7.71 (s, 1H), 7.30–7.37 (m, 2H), 7.22–7.26 (m, 2H), 7.07 (s, 1H), 6.02–6.06 (m, 1H), 5.32–5.34 (m, 1H), 5.20–5.23 (m, 1H), 4.85 (s, 2H), 3.70 (s, 3H). ESI-MS: 420.1 $[M+H]^+$.

***N*-(4-Fluoro-2-methoxy-5-nitrophenyl)-4-(1-(prop-2-yn-1-yl)-1H-indol-3-yl)pyrimidin-2-amine (3b-3).** Yield 66%, brown oil. ^{1}HNMR (400 MHz, CD_3OD): δ 8.30–8.33 (m, 2H), 7.80 (s, 1H), 7.57 (s, 1H), 7.38–7.41 (m, 1H), 7.20–7.22 (m, 2H), 7.14 (d, 1H), 7.05–7.07 (m, 1H), 4.94 (s, 2H), 3.66 (s, 3H), 2.31 (s, 1H). ESI-MS: 418.1 $[M+H]^+$.

2-(3-(2-((4-Fluoro-2-methoxy-5-nitrophenyl)amino)pyrimidin-4-yl)-*1H*-indol-1-yl)ethan-1-ol (3b-4). Yield 68%, brown foam. ^{1}HNMR (400 MHz, CD_3OD): δ 8.25 (d, 1H), 8.26–8.28 (m, 1H), 7.89 (s, 1H), 7.60 (s, 1H), 7.44–7.46 (m, 1H), 7.22–7.26 (m, 2H), 7.05–7.14 (m, 2H), 4.24 (t, 2H), 3.74 (t, 2H), 3.69 (s, 3H). ESI-MS: 424.1 $[M+H]^+$.

3-(2-((4-Fluoro-2-methoxy-5-nitrophenyl)amino)pyrimidin-4-yl)-*N*,N-dimethyl-1H-indole-1-sulfonamide (3b-5). Yield 44%, brown foam. ^{1}HNMR (400 MHz, CD_3OD): δ 8.31–8.33 (m, 1H), 8.24–8.26 (m, 1H), 8.07–8.09 (m, 1H), 7.86 (s, 1H), 7.71–7.75 (m, 1H), 7.41–7.46 (m, 2H), 7.16 (s, 1H), 7.07 (s, 1H), 3.69 (s, 3H), 2.70 (s, 6H). ESI-MS: 487.0 $[M+H]^+$.

1-(3-(2-((4-Fluoro-2-methoxy-5-nitrophenyl)amino)pyrimidin-4-yl)-*1H*-indol-1-yl)ethan-1-one (3b-6). Yield 70%, brown foam. ^{1}HNMR (400 MHz, CD_3OD): δ 8.34–8.37 (m, 2H), 7.98–8.00 (m, 1H), 7.89 (s, 1H), 7.49–7.53 (m, 3H), 7.43 (d, 1H), 7.07 (s, 1H), 3.69 (s, 3H), 2.44 (s, 3H). ESI-MS: 422.0 $[M+H]^+$.

***N*-(4-Fluoro-2-methoxy-5-nitrophenyl)-4-(1-(oxetan-3-yl)-1H-indol-3-yl)pyrimidin-2-amine (3b-7).** Yield 60%, brown foam. ^{1}HNMR (400 MHz, CD_3OD): δ 8.33 (d, 1H), 8.25 (d, 1H), 7.86 (s, 1H), 7.63 (s, 1H), 7.28–7.30 (m, 1H), 7.18–7.20 (m, 2H), 7.09–7.13 (m, 2H), 5.06–5.08 (m, 1H), 4.86–4.90 (m, 4H), 3.70 (s, 3H). ESI-MS: 436.1 $[M+H]^+$.

*4.4. General procedure for the synthesis of compounds **5a-1, 5a-2, 5b-1~5b-7***

Compound **3** (1 mmol) and N,N,N′-trimethylethane-1,2-diamine (1 mmol) were dissolved in 20 mL of DMA and the obtained solution was heated to 140 °C and stirred for 5 h. thereafter, the solvent was removed under reduced pressure; the residue was dissolved in MeOH, to which catalytic amount of Pd/C was added. With the input of H_2 gas the reaction mixture was kept stirring for 3 h. Then the mixture was filtrated and the product was obtained via column chromatography (CH_2Cl_2: CH_3OH = 10: 1).

***N4*-(4-(1-Cyclopropyl-*1H*-indol-3-yl)-5-(trifluoromethyl)pyrimidin-2-yl)-*N1*-(2-(dimethylamino) ethyl)-5-methoxy-*N1*-methylbenzene-1,2,4-triamine (5a-1).** Yield 50%, brown oil. ^{1}HNMR (400 MHz, CD_3OD): δ 8.50–8.55 (m, 2H), 7.06–7.17 (m, 4H), 6.41 (s, 1H), 6.08 (s, 1H), 3.48 (s, 3H), 3.16–3.18 (m, 2H), 2.94–2.96 (m, 1H), 2.86 (s, 3H), 2.42–2.44 (m, 2H), 2.18 (s, 6H), 1.14–1.29 (m, 4H). ESI-MS: 540.3 $[M+H]^+$.

***N1*-(2-(Dimethylamino)ethyl)-5-methoxy-*N1*-methyl-*N4*-(4-(1-(oxetan-3-yl)-1H-indol-3-yl)-5-(trifluoromethyl)pyrimidin-2-yl) benzene-1,2,4-triamine (5a-2).** Yield 55%, yellow oil. ^{1}HNMR (400 MHz, CD_3OD): δ 8.73 (s, 1H), 8.47–8.49 (m, 1H), 7.41 (s, 1H), 7.27–7.35 (m, 2H), 7.09–7.11 (m, 1H), 6.40 (s, 1H), 6.11 (s, 1H), 4.96–4.98 (m, 1H), 4.84–4.88 (m, 4H), 3.48 (s, 3H), 3.15–3.18 (m, 2H), 2.88 (s, 3H), 2.42–2.44 (m, 2H), 2.18 (s, 6H). ESI-MS: 556.2 $[M+H]^+$.

***N4*-(4-(1-Cyclopropyl-1H-indol-3-yl)pyrimidin-2-yl)-*N1*-(2-(dimethylamino)ethyl)-5-methoxy-*N1*-methylbenzene-1,2,4-triamine (5b-1).** Yield 53%, orange oil. ^{1}HNMR (400 MHz, CD_3OD): δ 8.28–8.30 (m, 1H), 8.11–8.12 (m, 1H), 7.34 (s, 1H), 7.09–7.15 (m, 2H), 7.01–7.04 (m, 2H), 6.41 (s, 1H), 6.10 (s, 1H), 3.48 (s, 3H), 3.15–3.18 (m, 2H), 2.94–2.96 (m, 1H), 2.88 (s, 3H), 2.42–2.44 (m, 2H), 2.18 (s, 6H), 1.19–1.27 (m, 4H). ESI-MS: 472.2 $[M+H]^+$.

***N4*-(4-(1-Allyl-*1H*-indol-3-yl)pyrimidin-2-yl)-*N1*-(2-(dimethylamino)ethyl)-5-methoxy-*N1*-methylbenzene-1,2,4-triamine (5b-2).** Yield 51%, brown oil. ^{1}HNMR (400 MHz, CD_3OD): δ 8.33–8.39 (m, 2H), 7.71 (s, 1H), 7.22–7.35 (m, 4H), 6.41 (s, 1H), 6.02–6.08 (m, 2H), 5.23–5.31 (m, 2H), 4.86 (br, 2H), 3.45 (s, 3H), 3.15–3.17 (m, 2H), 2.88 (s, 3H), 2.42–2.44 (m, 2H), 2.18 (s, 6H). ESI-MS: 472.2 $[M+H]^+$.

***N1*-(2-(Dimethylamino)ethyl)-5-methoxy-*N1*-methyl-N4-(4-(1-(prop-2-yn-1-yl)-1H-indol-3-yl)pyrimidin-2-yl)benzene-1,2,4-triamine (5b-3).** Yield 78%, yellow oil. ^{1}HNMR (400 MHz, CD_3OD): δ 8.37–8.41 (m, 2H), 7.51 (s, 1H), 7.36–7.38 (m, 1H), 7.14–7.20 (m, 3H), 6.38 (s, 1H), 6.11 (s, 1H), 4.95 (s, 2H), 3.46 (s, 3H), 3.15–3.17 (m, 2H), 2.85 (s, 3H), 2.42–2.44 (m, 2H), 2.30 (s, 1H), 2.18 (s, 6H). ESI-MS: 470.2 $[M+H]^+$.

2-(3-(2-((5-Amino-4-((2-(dimethylamino)ethyl)(methyl)amino)-2-methoxyphenyl)amino) pyrimidin-4-yl)-*1H*-indol-1-yl) ethan-1-ol (5b-4). Yield 50%, brown oil. ^{1}HNMR (400 MHz, CD_3OD): δ 8.27–8.31 (m, 2H), 7.66 (s, 1H), 7.44–7.46 (m, 1H), 7.25–7.28 (m, 1H), 7.15–7.20 (m, 2H), 6.40 (s, 1H), 6.10 (s, 1H), 4.29 (t, 2H), 3.74 (t, 2H), 3.45 (s, 3H), 3.15–3.18 (m, 2H), 2.88 (s, 3H), 2.42–2.44 (m, 2H), 2.18 (s, 6H). ESI-MS: 476.2 $[M+H]^+$.

3-(2-((5-Amino-4-((2-(dimethylamino)ethyl)(methyl)amino)-2-methoxyphenyl)amino)pyrimidin-4-yl)-*N*,N-dimethyl-1H-indole-1-sulfonamide (5b-5). Yield 41%, brown oil. ^{1}HNMR (400 MHz, CD_3OD): δ 8.30–8.35 (m, 2H), 8.07–8.09 (m, 1H), 7.73–7.75 (m, 1H), 7.41–7.46 (m, 2H), 7.15 (s, 1H), 6.44 (s, 1H), 6.12 (s, 1H), 3.48 (s, 3H), 3.15–3.18 (m, 2H), 2.88 (s, 3H), 2.79 (s, 6H), 2.43–2.47 (m, 2H), 2.21 (s, 6H). ESI-MS: 539.2 $[M+H]^+$.

1-(3-(2-((5-Amino-4-((2-(dimethylamino)ethyl)(methyl)amino)-2-methoxyphenyl)amino) pyrimidin-4-yl)-*1H*-indol-1-yl) ethan-1-one (5b-6). Yield 40%, brown oil. ^{1}HNMR (400 MHz, CD_3OD): δ 8.30 (d, 1H), 7.97–8.01 (m, 2H), 7.43–7.53 (m, 4H), 6.35 (s, 1H), 6.02 (s, 1H), 3.48 (s, 3H), 3.15–3.18 (m, 2H), 2.88 (s, 3H), 2.58 (s, 3H), 2.43–2.47 (m, 2H), 2.20 (s, 6H). ESI-MS: 474.2 $[M+H]^+$.

***N1*-(2-(dimethylamino)ethyl)-5-methoxy-*N1*-methyl-*N4*-(4-(1-(oxetan-3-yl)-*1H*-indol-3-yl)pyrimidin-2-yl)benzene-1,2,4-triamine (5b-7).** Yield 48%, yellow oil. ^{1}HNMR (400 MHz, CD_3OD): δ 8.26–8.31 (m, 2H), 7.63 (s, 1H), 7.20–7.26 (m, 3H), 7.09–7.11 (m, 1H), 6.44 (s, 1H), 6.06 (s, 1H), 4.96–4.98 (m, 1H), 4.84–4.88 (m, 4H), 3.49 (s, 3H), 3.15–3.18 (m, 2H), 2.88 (s, 3H), 2.43–2.47 (m, 2H), 2.20 (s, 6H). ESI-MS: 488.3 $[M+H]^+$.

*4.5. General procedure for the synthesis of compounds **6a-1, 6a-2, 6b-1~6b-7***

Compound **5** (1 mmol) and DIPEA (1.1 mmol) were added into 20 mL of THF and the obtained solution was cooled to 0 °C. Then acryloyl chloride (1.1 mmol) was added dropwise. The reaction solution was stirred for 5 h. Thereafter, the solvent was removed under reduced pressure and the product was obtained via column chromatography (CH_2Cl_2: CH_3OH = 10: 1).

***N*-(5-((4-(1-Cyclopropyl-1H-indol-3-yl)-5-(trifluoromethyl)pyrimidin-2-yl)amino)-2-((2-(dimethylamino)ethyl)(methyl)amino)-4-methoxyphenyl)acrylamide (6a-1).** Yield 90%, yellow oil. ^{1}HNMR (400 MHz, CD_3OD): δ 8.46 (d, 1H), 8.35–8.37 (m, 1H), 7.09–7.18 (m, 4H), 6.29–6.42 (m, 3H), 6.13 (s, 1H), 5.65–5.67 (m, 1H), 3.49 (s, 3H), 3.16–3.18 (m, 2H), 2.94–2.97 (m, 2H), 2.86 (s, 3H), 2.42–2.45 (m, 2H), 2.18 (s, 6H), 1.14–1.29 (m, 4H). ^{13}CNMR (100 MHz, CD_3OD): δ 165.4, 164.2, 163.3 (q), 156.9 (q), 139.2, 137.4, 136.8, 135.8, 133.7, 132.9, 130.0, 129.8, 123.3, 122.5, 120.7, 120.6, 120.1 (q), 119.2 (q), 116.5, 109.7, 101.0, 100.1, 55.6, 53.2, 50.5, 45.6 (2C), 40.2, 28.4, 7.7 (2C). HR-MS(ESI) calcd for $[M+H]^+$ = 594.2726, found 594.2732.

***N*-(2-((2-(Dimethylamino)ethyl)(methyl)amino)-4-methoxy-5-((4-(1-(oxetan-3-yl)-*1H*-indol-3-yl)-5-(trifluoromethyl)pyrimidin-2-yl)amino)phenyl)acrylamide (6a-2).** Yield 88%, yellow foam. ^{1}HNMR (400 MHz, CD_3OD): δ 8.73 (s, 1H), 8.48–8.50 (m, 1H), 8.46 (s, 1H), 7.24–7.33 (m, 2H), 7.16 (s, 1H), 7.09–7.13 (m, 1H), 6.29–6.36 (m, 2H), 6.16 (s, 1H), 5.64–5.67 (m, 1H), 4.95–4.99 (m, 1H), 4.82–4.86 (m, 4H), 3.47 (s, 3H), 3.01–3.04 (m, 2H), 2.94–2.97 (m, 2H), 2.76 (s, 3H), 2.42–2.45 (m, 2H), 2.18 (s, 6H). ^{13}CNMR (100 MHz, CD_3OD): δ 164.2, 162.1, 160.8 (q), 155.5 (q), 139.2, 138.4, 136.7, 136.5, 133.7, 131.7, 130.0, 129.8, 123.5, 122.3, 120.5, 120.0 (q), 118.3 (q), 115.3, 110.9, 101.0, 100.2, 71.4 (2C), 55.6, 53.2, 53.0, 50.5, 40.5 (2C), 40.2. HR-MS (ESI) calcd for $[M+H]^+$ = 610.2675, found 610.2670.

***N*-(5-((4-(1-cyclopropyl-*1H*-indol-3-yl)pyrimidin-2-yl)amino)-2-((2-(dimethylamino)ethyl) (methyl)amino)-4-methoxyphenyl) acrylamide (6b-1).** Yield 85%, yellow oil. ^{1}HNMR (400 MHz, CD_3OD): δ 8.28–8.31 (m, 1H), 8.11 (d, 1H), 7.11–7.30 (m, 4H), 7.02 (d, 1H),

6.29–6.39 (m, 3H), 6.13–6.17 (m, 1H), 5.65–5.67 (m, 1H), 3.49 (s, 3H), 2.94–2.97 (m, 2H), 2.76 (s, 3H), 2.42–2.45 (m, 2H), 2.18 (s, 6H), 1.14–1.29 (m, 4H). ^{13}CNMR (100 MHz, $CDCl_3$): δ 166.1, 164.2, 161.6, 158.6, 139.2, 136.2, 135.2, 134.8, 133.7, 130.0, 129.8, 129.4, 121.3, 121.2, 120.8, 120.6, 116.3, 114.5, 109.7, 101.1, 100.2, 55.6, 53.2, 50.5, 45.6 (2C), 40.2, 28.4, 7.7 (2C). HR-MS(ESI) calcd for $[M+H]^+$ = 526.2852, found 526.2860.

***N*-(5-((4-(1-allyl-1H-indol-3-yl)pyrimidin-2-yl)amino)-2-((2-(dimethylamino)ethyl)(methyl) amino)-4-methoxyphenyl)acrylamide (6b-2).** Yield 85%, yellow oil. ^{1}HNMR (400 MHz, CD_3OD): δ 8.33–8.39 (m, 2H), 7.71 (s, 1H), 7.16–7.35 (m, 5H), 6.29–6.39 (m, 2H), 6.06–6.15 (m, 2H), 5.65–5.67 (m, 1H), 5.23–5.34 (m, 2H), 4.85–4.86 (m, 1H), 3.48 (s, 3H), 3.00–3.02 (m, 2H), 2.75 (s, 3H), 2.42–2.45 (m, 2H), 2.18 (s, 6H). ^{13}CNMR (100 MHz, CD_3OD): δ 164.5, 164.2, 160.2, 157.2, 139.3, 139.2, 135.8, 134.8, 133.7, 132.7, 130.0, 129.8, 129.6, 121.8, 121.3, 120.8, 119.8, 119.5, 114.6, 110.6, 109.4, 101.1, 100.2, 55.6, 53.2, 51.2, 50.5, 45.6 (2C), 40.2. HR-MS(ESI) calcd for $[M+H]^+$ = 526.2852, found 526.2847.

***N*-(2-((2-(Dimethylamino)ethyl)(methyl)amino)-4-methoxy-5-((4-(1-(prop-2-yn-1-yl)-*1H*-indol-3-yl)pyrimidin-2-yl)amino) phenyl)acrylamide (6b-3).** Yield 88%, yellow foam. ^{1}HNMR (400 MHz, CD_3OD): δ 8.33–8.34 (m, 2H), 7.57 (s, 1H), 7.38–7.40 (m, 1H), 7.13–7.21 (m, 4H), 6.36–6.39 (m, 1H), 6.13–6.25 (m, 2H), 5.65–5.67 (m, 1H), 4.95 (s, 1H), 3.48 (s, 3H), 3.00–3.02 (m, 2H), 2.75 (s, 3H), 2.42–2.45 (m, 2H), 2.23 (s, 1H), 2.18 (s, 6H). ^{13}CNMR (100 MHz, CD_3OD): δ 164.2, 164.0, 160.2, 157.2, 139.4, 139.2, 138.8, 134.8, 133.7, 131.4, 130.0, 129.8, 121.6, 121.3, 120.8, 119.3, 114.5, 112.4, 108.0, 101.1, 100.2, 79.3, 77.9, 55.6, 53.2, 50.5, 45.6 (2C), 40.2, 38.4. HR-MS(ESI) calcd for $[M+H]^+$ = 524.2696, found 524.2690.

***N*-(2-((2-(Dimethylamino)ethyl)(methyl)amino)-5-((4-(1-(2-hydroxyethyl)-*1H*-indol-3-yl)pyrimidin-2-yl)amino)-4-methoxyphenyl)acrylamide (6b-4).** Yield 91%, yellow oil. ^{1}HNMR (400 MHz, CD_3OD): δ 8.27–8.34 (m, 2H), 7.61 (s, 1H), 7.42–7.44 (m, 1H), 7.25–7.28 (m, 1H), 7.13–7.20 (m, 3H), 6.36–6.39 (m, 1H), 6.27 (s, 1H), 6.13–6.17 (m, 1H), 5.65–5.67 (m, 1H), 4.29 (t, 2H), 3.74 (t, 2H), 3.48 (s, 3H), 3.00–3.02 (m, 2H), 2.75 (s, 3H), 2.42–2.45 (m, 2H), 2.18 (s, 6H). ^{13}CNMR (100 MHz, CD_3OD): δ 164.2, 163.8, 160.2, 157.2, 139.5, 139.2, 136.7, 134.8, 133.7, 130.0, 129.8, 128.1, 121.6, 121.4, 120.8, 119.1, 114.8, 110.9, 109.1, 101.1, 100.2, 61.0, 55.6, 54.3, 53.2, 50.5, 45.6 (2C), 40.2. HR-MS(ESI) calcd for $[M+H]^+$ = 530.2801, found 530.2810.

***N*-(2-((2-(Dimethylamino)ethyl)(methyl)amino)-5-((4-(1-(N,N-dimethylsulfamoyl)-*1H*-indol-3-yl)pyrimidin-2-yl)amino)-4-methoxyphenyl)acrylamide (6b-5).** Yield 80%, brown oil. ^{1}HNMR (400 MHz, CD_3OD): δ 8.30 (d, 1H), 8.23–8.26 (m, 1H), 8.07–8.09 (m, 1H), 7.72–7.74 (m, 1H), 7.37–7.46 (m, 2H), 7.18 (s, 1H), 7.15 (s, 1H), 6.36–6.39 (m, 1H), 6.27 (s, 1H), 6.13–6.17 (m, 1H), 5.65–5.67 (m, 1H), 3.48 (s, 3H), 3.00–3.02 (m, 2H), 2.82 (s, 6H), 2.75 (s, 3H), 2.42–2.45 (m, 2H), 2.18 (s, 6H). ^{13}CNMR (100 MHz, CD_3OD): δ 164.2, 163.8, 161.6, 158.6, 139.2, 138.3, 134.8, 134.2, 133.9, 133.7, 130.0, 129.8, 125.1, 123.6, 120.8, 119.5, 118.4, 117.0, 107.5, 101.1, 100.2, 55.6, 53.2, 50.5, 45.6 (2C), 38.3 (2C). HR-MS(ESI) calcd for $[M+H]^+$ = 593.2580, found 593.2588.

***N*-(5-((4-(1-Acetyl-1H-indol-3-yl)pyrimidin-2-yl)amino)-2-((2-(dimethylamino)ethyl) (methyl)amino)-4-methoxyphenyl)acrylamide (6b-6).** Yield 90%, yellow oil. ^{1}HNMR (400 MHz, CD_3OD): δ 8.35–8.37 (m, 2H), 7.98–7.99 (m, 1H), 7.43–7.50 (m, 3H), 7.16 (s, 1H), 6.36–6.39 (m, 1H), 6.28 (s, 1H), 6.13–6.17 (m, 1H), 5.65–5.67 (m, 1H), 3.48 (s, 3H), 3.00–3.02 (m, 2H), 2.75 (s, 3H), 2.42–2.45 (m, 2H), 2.40 (s, 1H), 2.18 (s, 6H). ^{13}CNMR (100 MHz, CD_3OD): δ 168.1, 165.1, 164.2, 160.6, 157.6, 139.2, 137.9, 134.8, 133.9, 133.7, 130.6, 130.0, 129.8, 125.6, 125.4, 120.8, 119.0, 117.6, 114.8, 114.6, 101.1, 100.2, 55.6, 53.2, 50.5, 45.6 (2C), 40.2, 24.0. HR-MS(ESI) calcd for $[M+H]^+$ = 528.2645, found 528.2648.

***N*-(2-((2-(Dimethylamino)ethyl)(methyl)amino)-4-methoxy-5-((4-(1-(oxetan-3-yl)-*1H*-indol-3-yl)pyrimidin-2-yl)amino)phenyl) acrylamide (6b-7).** Yield 88%, yellow oil. ^{1}HNMR (400 MHz, CD_3OD): δ 8.45 (d, 1H), 8.25 (d, 1H), 7.60 (s, 1H), 7.14–7.28 (m, 4H), 6.26–6.38 (m, 4H), 5.64–5.67 (m, 1H), 4.95–4.98 (m, 1H), 4.82–4.87 (m, 4H), 3.52 (s, 3H), 3.00–3.02 (m, 2H), 2.78 (s, 3H), 2.42–2.45 (m, 2H), 2.21 (s, 6H). ^{13}CNMR (100 MHz, CD_3OD): δ 164.2, 163.4, 160.2, 157.2, 139.2, 137.5, 135.9, 134.8, 133.7, 130.0, 129.8, 128.2, 121.5, 121.0, 120.8, 120.5, 114.8, 113.4, 110.9, 101.1, 100.2, 71.4 (2C), 55.6, 53.2, 53.0, 50.5, 45.6 (2C), 40.2. HR-MS(ESI) calcd for $[M+H]^+$ = 542.2801, found 542.2808.

***In vitro* enzymatic assay** Homogeneous time-resolved fluorescent kinase assays were used to determine the inhibitory effect of the target compounds on EGFR wild-type and recombinant *N*-terminal GST-tagged human EGFR (T790M/L858R double-mutant enzymes). Generally, EGFR wild-type and double-mutant enzymes and the HTRF tyrosine kinase biotinylated substrate were treated with the tested compounds at five different concentrations (10-fold dilution steps, starting from 10 μM) in enzymatic buffer. Kinase activity assays were performed in a total reaction volume of 3 μL per well. A 1.5 μL enzyme reaction consisted of 1.6 nM EGFR (T970M, L858R), 1 mM DTT, and 10 mM $MgCl_2$. A 1.5 μL substrate mix consisted of 1 μM TK substrate, 1.6 μM ATP, 1 mM DTT, and 10 mM $MgCl_2$. After the enzymatic reaction was started and allowed to last 30 min at room temperature, the detection reagents was added to stop the reaction. The detection step continued for 1 h, and then the IC_{50} values were calculated using GraphPad Prism 8. Three independent experiments were performed for each concentration.

Molecular docking study. Homology modeling was carried out by the MOE (Molecular Operating Environment) software (Chemical Computing Group Inc.) using our former reported method.[16] Initial minimization was performed within the homology modeling function of MOE. The model from MOE was minimized with a few thousand cycles of minimization using the ABNR (adopted-basis Newton-Raphson) method. Ligands were modeled by positioning them in the active site in accordance with the published crystal structures (PDB code: 4ZAU and 6JX4). The entire complex was then subjected to alternate cycles of minimization and dynamics. Each dynamics run was short, about 3 ps. The intent was to get a satisfactory structure for the complex that was consistent with the published crystal structure.

***In vitro* cellular assays** H1975 and A431 cell lines were used for the cell proliferation assays. In this experiment, the inhibitory effect of the compound on the proliferation of experimental cells was tested by CellTiter-Glo method, and the IC_{50} of the compound inhibiting cell proliferation activity was obtained as following: Inoculate 50–100 μL of experimental cell suspension in a 96-well cell culture plate at a density of 1–5 × 10^4 cells/mL, and place the plate in an incubator for 16–24 h (37 °C, 5% CO_2). Then add a gradient dilution of the solution of the compound (five different concentrations, 10-fold dilution steps starting from 10 μM) to be tested to the culture plate, and incubate the plate for 72 h (37 °C, 5% CO_2) in the incubator. Add 50–100 μL CellTiter-Glo reagent to each well, shake at room temperature or let stand for 5–30 min. Determination of the chemiluminescence signal value of each plate by a microplate reader, then calculate the inhibition rate by the value of the chemiluminescence signal and the IC_{50} of the compound is obtained by curve fitting according to the inhibition rates of different concentrations.

Western blotting assay Treatment of 3 nude mice with subcutaneous xenograft H1975 tumor with 5 mg tested compounds via single intragastric administration respectively, blood and tumor tissues were taken after 6 h. Tumor tissue was washed by using D-Hanks Buffer three times and cut into 4 mm pieces, and then treated with trypsin/collagenase to turn into cell suspensions which were dispersed in solution, and finally split. The samples were then performed WB analysis to detect phosphorylated EGFR and the downstream phosphor-Akt and phosphor-Erk levels.

***In Vivo* Efficacy Study** BALB/c nude mice were subcutaneously inoculated with 0.1 mL of experimental cell suspension (7 × 10^7/ml) to establish a subcutaneous xenograft model. When the tumors were grown to an average volume of 200–250 mm^3, they were randomly administered according to tumor size and mouse body weight. Tumor volume

was measured twice a week, and the weight of tumor-bearing mice was weighed twice a day, and data were recorded. After 11 days of administration, the tumor tissue was taken and weighed, and photographed at the same time. The T/C values were calculated according to the National Cancer Institute (NCI) standardized transplant tumor evaluation method.

Pharmacokinetic Assay Using our former reported method,[17] rats, half male and half female for 6–7 weeks, are purchased from Shanghai SLAC Laboratory Animal CO. LTD; feed the rats under grade SPF. Rats were intragastrically administered, fasted for not less than 12 h before administration, free to drink water, and fed for 4 h after administration. Blood samples were taken from the posterior ocular veins before administration and 5 min, 0.25, 0.5, 1.0, 2.0, 4.0, 6.0, 10 and 24 h after administration. Determination of **6b-1** and its metabolite **9** in rat plasma by LC-MS and the pharmacokinetic parameters of rats were calculated using the non-compartmental model of Phoenix WinNonlin 6.4 software (Pharsight, USA).

Declaration of Competing Interest

The authors declare that they have no known competing financial interests or personal relationships that could have appeared to influence the work reported in this paper.

Acknowledgments

The work is supported by the Fundamental Research Funds for the Central Universities. Dr. Fang is thankful to the support of the State Key Laboratory for Chemistry and Molecular Engineering of Medicinal Resources (Guangxi Normal University) (CMEMR2017-B05), “Qing-Lan” project in Colleges and Universities of Jiangsu Province, the National Science and Technology Major Foundation of China, and the Priority Academic Program Development of Jiangsu Higher Education Institutions. We thank China Pharmaceutical University for the software support. The authors also thank Dr. C. Sun and Jiangsu Hansoh Pharmaceutical Corporation for the valuable help on the chemistry and pharmacology work.

References

1 Han JY, Park K, Kim SW, et al. *J Clin Oncol*. 2012;30:1122.
2 Yu HA, Arcila ME, Rekhtman N, et al. *Clin Cancer Res*. 2013;19:2240.
3 Michalczyk A, Klueter S, Rode HB, et al. *Bioorg Med Chem*. 2008;16:3482.
4 Kobayashi S, Boggon TJ, Jänne PA, et al. *N Engl J Med*. 2005;352:786.
5 Yoo SB, Kim YJ, Kim H, et al. *Ann Surg Oncol*. 2013;20:545.
6 Ward RA, Anderton MJ, Ashton S, et al. *J Med Chem*. 2013;56:7025.
7 Finlay MR, Anderton M, Ashton S, et al. *J Med Chem*. 2014;57:8249.
8 Tjin Tham Sjin R, Lee K, Walter AO, et al. *J Mol Cancer Ther*. 2014;13:1468.
9 Cross DA, Ashton SE, Ghiorghiu S, et al. *Cancer Discov*. 2014;4:104.
10 Dickinson PA, Cantarini MV, Collier J, et al. *Drug Metab Dispos*. 2016;44:1201.
11 Gaber AA, Bayoumi AH, El-Morsy AM, Sherbiny FF, Mehany ABM, Eissa IH. *Bioorg Chem*. 2018;80:375.
12 Elmetwally SA, Saied KF, Eissa IH, Elkaeed EB. *Bioorg Chem*. 2019;88, 102944.
13 Nasser AA, Eissa IH, Oun MR, et al. *Org Biomol Chem*. 2020;18:7608.
14 Lategahn J, Keul M, Klövekorn P, et al. *Chem Sci*. 2019;10:10789.
15 Chen C, Cheng T, Han CH, Huang ZQ, Pan T. *Asian J Chem*. 2013;25:10325.
16 Fang L, Chen M, Liu Z, Fang X, Gou S, Chen L. *Bioorg Med Chem*. 2016;24:886.
17 Liu Y, Xia Q, Fang L. *Bioorg Med Chem*. 2018;26:3992.